HHS Public Access

Author manuscript

Eur Radiol. Author manuscript; available in PMC 2023 December 01.

Published in final edited form as:

Eur Radiol. 2022 December ; 32(12): 8748–8760. doi:10.1007/s00330-022-08894-1.

Temporal assessment of lesion morphology on radiological images beyond lesion volumes – A proof-of-principle study

Márton Kolossváry, MD, PhD[a], **David A Bluemke, MD**[b], **Elliot K. Fishman, MD**[c], **Gary Gerstenblith, MD**[d], **David Celentano, ScD**[e], **Raul N. Mandler, MD**[f], **Jag Khalsa, PhD**[g], **Sandeepan Bhatia, MD**[g], **Shaoguang Chen, MS**[g], **Shenghan Lai, MPH**[a,c,d,e,g], **Hong Lai, PhD**[c,g]

[a]Department of Pathology, Johns Hopkins University School of Medicine; 600 N Wolfe St, Baltimore, MD, USA, 21287

[b]University of Wisconsin School of Medicine and Public Health; 750 Highland Ave, Madison, WI, USA, 53726

[c]Department of Radiology, Johns Hopkins University School of Medicine; 601 N Caroline St, Baltimore, MD, USA, 21205

[d]Department of Medicine, Johns Hopkins University School of Medicine; 733 N Broadway, Baltimore, MD, USA, 21205

[e]Department of Epidemiology, Johns Hopkins University Bloomberg School of Public Health; 614 Wolfe N Wolfe St, Baltimore, MD, USA, 21205

[f]National Institute on Drug Abuse, National Institutes of Health, Bethesda, MD, 10 Center Dr, Bethesda, MD, USA, 20814

[g]Institute of Human Virology, University of Maryland School of Medicine, 725 W Lombard Street, Baltimore, MD, USA, 21201

Abstract

Objectives: To develop a general framework to assess temporal changes in lesion morphology on radiological images beyond volumetric changes, and to test whether cocaine abstinence changes coronary plaque structure on serial coronary CT angiography (CTA).

Methods: Chronic cocaine users with human immunodeficiency virus (HIV) infection were prospectively enrolled to undergo cash-based contingency management to achieve cocaine abstinence. Participants underwent coronary CTA at baseline, 6- and 12-months following recruitment. We segmented all coronary plaques and extracted 1103 radiomic features. We implemented weighted correlation network analysis to derive consensus eigen radiomic features (named as different colors) and used linear mixed models and mediation analysis to assess whether cocaine abstinence affects plaque morphology correcting for clinical variables and plaque volumes and whether serum biomarkers causally mediate these changes. Furthermore, we used Bayesian hidden Markov network changepoint analysis to assess potential rewiring of the radiomic network.

Address of correspondence: Name: Shenghan Lai, Address: Institute of Human Virology, 725 W Lombard St, Baltimore, MD, USA, 21201, Tel: (1) 410-706-7192, slai@ihv.umaryland.edu.

Results: 69 PLWH (median age 55 IQR: 52-59 years, 19% female) completed the study, of whom 26 achieved total abstinence. 20 consensus eigen radiomic features were derived. Cocaine abstinence significantly affected the pink and cyan eigen features (−0.04 CI: [−0.06; −0.02], p=0.0009; 0.03 CI: [0.001; 0.04], p=0.0017, respectively). These effects were mediated through changes in Endothelin-1 levels. In abstinent individuals we observed significant rewiring of the latent radiomic signature network.

Conclusions: Using our proposed framework, we found 1 year cocaine abstinence to significantly change specific latent coronary plaque morphological features and rewire the latent morphologic network above and beyond changes in plaque volumes and clinical characteristics.

Keywords

Artificial Intelligence; Longitudinal Studies; Coronary Artery Disease; Cocaine Addiction; Precision Medicine

INTRODUCTION

Advancements in medical therapies has made it increasingly difficult to demonstrate the effectiveness of new drugs above and beyond current standards of care [1]. Therefore, surrogate imaging markers of hard clinical end-points are utilized to assess the efficacy of new interventions [2; 3]. In the case of coronary atherosclerosis, coronary computed tomography angiography (CTA) provides a non-invasive imaging modality to monitor volumetric plaque changes in-vivo [4]. Coronary CTA measured plaque volumes are increasingly being used as surrogate markers of drug efficacy in clinical trials [5; 6], as changes in plaque volumes have been shown to have additive predictive value beyond clinical assessment in predicting major adverse cardiac events [7]. However, morphological changes in pathologies above and beyond changes in lesion volumes are equally important [8], but visual assessment of morphological characteristics does not allow quantitative temporal assessment.

Radiomics is the process of extracting quantitative imaging markers describing the structure and composition of a lesion using numerical values [9; 10]. These parameters have been shown to correlate well with adverse plaque characteristics and provide an alternative to quantitatively identify vulnerable coronary plaques [11; 12]. Furthermore, studies have shown that radiomics can extract information regarding plaque morphology that visual assessment is unable to recognize, therefore providing a framework for precision phenotyping of coronary artery disease (CAD) [13; 14]. However, radiomic features are highly redundant as they are numerical representations of around 10-50 latent features [11; 15]. In the case of longitudinal data analysis, intra-individual changes in parameter values are used to assess the potential effect of a predictor on the outcome. Therefore, robust estimates of the underlying latent morphology at each time point are needed.

Chronic cocaine use has been shown to significantly increase coronary plaque burden [16; 17]. A pilot investigation has also shown that cocaine abstinence results in noncalcified plaque regression [18]. However, it is unknown whether cocaine abstinence changes coronary plaque morphology beyond its effects on plaque volumes.

In this study, we propose a general framework for the temporal assessment of morphological changes in pathologies on radiological images. As a proof-of-principle, we wished to assess whether we can detect morphological changes in coronary atherosclerosis following cocaine abstinence above and beyond its documented effects on plaque volume among individuals with human immunodeficiency virus (HIV) infection undergoing cash-based contingency management intervention.

MATERIALS AND METHODS

Study participants

The institutional review board approved the study protocol, and all study participants provided written informed consent. All procedures used in this study followed the Health Insurance Portability and Accountability Act, local and federal regulations, and the Declaration of Helsinki.

Between March 2014 and August 2016, 100 chronic cocaine users were consecutively enrolled from a prospective epidemiologic observational study investigating the effects of HIV, cocaine use, and other associated factors on CAD into the current cash-based contingency management intervention [17; 19]. Detailed study protocol has been published earlier [18]. In brief, inclusions criteria into the current analysis were: (1) being HIV-infected, (2) previous coronary CTA-confirmed subclinical atherosclerosis, and (3) current cocaine use confirmed by a positive urine test for cocaine or benzoylecgonine during the initial screening interview and self-reported use by any route for at least 6 months, administered at least 4 times a month. Exclusion criteria included (1) obstructive CAD (>70% stenosis) on coronary CTA or any symptoms believed to be related to cardiovascular disease, (2) history of serious physical disease or current physical disease (eg severe trauma or cancer), (3) infrequent cocaine users (fewer than 4 times a month in the last consecutive 6 months), (4) pregnancy, (5) chronic kidney disease with an estimated glomerular filtration rate of <60 mL/min/1.73m^2, and (6) contraindication to CTA scans, including a history of contrast allergy.

Cash-based contingency management intervention

Details of the cash-based contingency management protocol have been published previously [18]. Briefly, the proposed cash-based contingency management protocol systematically reinforces cocaine abstinence by using an escalating cash incentive program, where participants receive an increasing number of points (1 point=$1) for negative cocaine test results. Cocaine abstinence was defined as providing no positive urine test during the 1-year period.

Coronary CTA procedures

Details of the CT scanning procedures have been described [17; 19], and are present in supplementary material.

Coronary CTA segmentation and radiomic feature calculations

Details are provided in supplemental material. In brief, plaque analysis was performed independently in the Department of Radiology and Imaging Sciences, NIH Clinical Center using dedicated software (QAngioCT, version 3.1.3.13; Medis Medical Imaging Systems) [20]. According to Hounsfield unit (HU) values, plaque volumes were further classified to low-attenuation noncalcified plaque volume: −100–30 HU noncalcified plaque volume: −100–350 HU and calcified plaque volume: ≥351 HU [21]. Segmented images were then loaded into the open-source Radiomics Image Analysis software package (v. 1.4.2; https://CRAN.R-project.org/package=RIA) in the R environment, where 1,103 radiomic features were calculated [11; 22].

Consensus eigen radiomic features

We propose a framework to calculate consensus eigen radiomic feature, based on weighted correlation network analysis (WGCNA) developed by Zhang et al [23].

Details regarding calculations are provided in supplemental material. In brief, following data pre-processing, a consensus topological overlap matrix (TOM) was calculated which describes the similarity network of the radiomic features considering all three timepoints. To cluster the radiomic features into consensus modules we used average linkage hierarchical clustering based on the consensus TOM-based dissimilarity. Then, we used the dynamic hybrid tree cut algorithm to identify the consensus radiomic modules [24]. Consensus eigen radiomic features are the first principal component of each module. All calculations were done using the WGCNA (v. 1.70-3) package in R [25].

Radiomic feature stability analysis

To assess whether consensus eigen radiomic features are robust to changes in the data, we conducted percolation analyses. Details of the analysis are presented in supplementary information.

Bayesian hidden Markov network changepoint model

To assess whether cocaine abstinence results in rewiring of the radiomic feature network beyond its effects on specific latent structural features, we conducted Bayesian hidden Markov network change models on the consensus eigen radiomic feature network at all three timepoints for abstinent and non-abstinent individuals [26]. Details of the analysis are presented in supplementary information.

Statistical Analysis

All continuous parameters were summarized by medians and interquartile ranges (IQRs), and all categorical parameters were summarized as frequencies and proportions. To compare differences between cocaine abstinent and non-abstinent individuals, Mann-Whitney U-test and the chi-square test was used for continuous and categorical variables respectively.

For descriptive purposes, patients were clustered using average linkage hierarchical clustering based on the raw radiomic feature values and compared using cophenetic correlation (dendextend (v. 1.15.1) package in R) [27].

Longitudinal data analysis was done considering all three examinations (baseline, 6-months, 12-months). We used linear mixed models including random intercepts and slopes for each individual [28; 29]. The models were corrected for sex, baseline age, and atherosclerosis cardiovascular disease (ASCVD) risk and time since baseline scan as these have all been reported to modulate the radiomic signature of CAD [15]. We also included noncalcified, calcified, and low-attenuation noncalcified plaque volumes at each visit to correct for any possible effect of cocaine abstinence on plaque components, and also to correct for inherent correlations between plaque volumes and radiomic features [15]. Linear mixed model analysis was done using the lme4 (v. 1.1-27) and lmerTest (v. 3.1-3) packages in R [30; 31].

We conducted causal mediation analysis using the mediate (v. 4.5.0) package [32], details are provided in supplemental material.

Due to the multiple comparisons being done, we applied Bonferroni correction. Our WGCNA analysis resulted in 20 consensus eigen radiomic features, therefore two-sided p values below 0.05/20 = 0.0025 were considered significant. All statistical calculations were done in the R environment (v. 4.0.0) [33]. All statistical code used for analysis and generating the images are available at: https://github.com/martonkolossvary/radiomics_temporal_assessment

RESULTS

Patient characteristics

Overall, 76 chronic cocaine users with HIV-infection began the cash-based contingency management intervention. From these individuals, 7 did not complete the contingency management or were lost to follow-up. Altogether, 69 people living with HIV completed the study, of whom 26 achieved total abstinence of cocaine use. The median age was 55 years (IQR: 52-59 years) and 19% were female. There was no significant difference in any anthropometric, clinical, laboratory, or plaque volume parameter between abstinent and non-abstinent individuals at the baseline visit ($p>0.05$ for all). Detailed baseline patient characteristics are presented in table 1.

Changes in patient hierarchical clustering dendrograms during follow-up

Based on missingness and zero variance criteria described in the supplemental methods, 2.0% (22/1,103) of radiomic features were removed from the analysis. Patients were clustered based on their normalized radiomic profiles using hierarchical clustering. The resulting patient clustering dendrograms and corresponding clinical characteristics and plaque volumes at baseline, 6-months, and 12-months are summarized in figure 1. Cophenetic correlation values between baseline and 6-months (*cophenetic correlation*=0.42), 6-months and 12-months (*cophenetic correlation*=0.67) show low correlation between the clustering dendrograms, indicating considerable changes in latent plaque morphology over the one-year period.

Scale free topology of the latent morphology network

Detailed results regarding the scale free topology of the radiomic network are presented in supplemental material. In brief, we found that similar to other biological networks the latent structural imaging feature network of coronary plaques follow an approximate scale free topology (supplementary figure 1).

Consensus radiomic feature modules and eigen radiomic features

Detailed results regarding consensus feature modules and eigen features are presented in supplementary material. In brief, we found 20 consensus radiomic modules (grey is used to mark features not allocated to any of the modules) in our dataset (figure 2a). These radiomic modules represent latent morphological coronary plaque features which are present in our data considering all three timepoints. The multidimensional scaling plot (figure 2b) shows that the radiomic features of the corresponding modules are situated apart from each other in a 3-dimensional latent space highlighting that the models represent different latent structural features. The mean of adjacencies, clustering coefficients, correlations, and maximum adjacency ratios regarding the three timepoints were high, indicating considerable inter-connectedness within the modules (figure 2c). These values were highly statistically different from random and higher than for the grey module, which represented radiomic features not assigned to any of the modules.

We derived consensus eigen radiomic features for each module using singular value decomposition of the corresponding radiomic expression matrix. Therefore, the imaging feature space of 3 timepoints x 1,081 features is reduced to 3 timepoints x 20 features. The eigen radiomic features were found to be good representations of the of each feature module, as the mean correlation between each corresponding feature and the eigen radiomic feature (mean module membership) was high for each module (range: 0.85-0.95; figure 2c). Furthermore, the eigen radiomic feature explained a high proportion of the variance of the corresponding features (range: 0.63-0.90; figure 2c).

Robustness analysis of the consensus eigen radiomic features

To conclude any results from consensus eigen radiomic features, first we need to be sure that our derived parameters of latent coronary plaque morphology are robust. Detailed results are presented in supplemental material. In brief, we found that even after removing 50% of the individuals or visits, the resulting hierarchical clustering dendrograms of the simulated data showed a mean cophenetic correlation >0.85 with the original data (figure 3a and 3b). Furthermore, we observed that that even after removing half of all patients or visits from our database, in both cases in 50% (10/20) of the modules the assigned features showed an 80% overlap with the originally assigned features (figure 3c and 3d). Most importantly, even after removing 50% of all patients or individuals, the derived eigen radiomic features corresponding to the reference network module assignment showed almost perfect correlation with the original eigen radiomic features with all Pearson correlation values above 0.99 (figure 3 e and 3f). All these results show that while the instability of individual radiomic features precludes them from being used to assess changes in plaque structure over time, our proposed methodology provides robust descriptors of latent structural phenotypes.

Effect of cocaine abstinence on temporal changes in atherosclerotic plaque structure

We choose linear mixed models as they provide a flexible approach to analyze temporal data and can handle missing data and model complex hierarchical data structures that may be present in clinical studies. After correcting for baseline age and ASCVD risk, sex, calcified, noncalcified, and low-attenuation noncalcified plaque volumes at each timepoint, cocaine abstinence was significantly associated with changes in the pink (p=0.0009) and the cyan (p=0.0017) consensus eigen radiomic features. Estimates of cocaine abstinence on all 20 consensus eigen radiomic features are presented in table 2.

Mediation analyses to assess which factors mediate the effects of cocaine abstinence

Detailed results are presented in supplemental material. In brief, for endothelin-1, we found the average causal mediation effect (ACME) to be significant for the pink consensus eigen radiomic feature (figure 4a; β=−0.01, 95% CI: −0.02–0.00, p=0.048) and also the cyan consensus eigen radiomic feature (figure 4c; β=0.01, 95% CI: 0.00–0.02, p=0.020), while the average direct effect (ADE) was non-significant in both cases (figure 4a and 4c; β=−0.01, 95% CI: −0.05–0.02, p=0.570; β=−0.02, 95% CI: −0.05–0.02, p=0.390; respectively). These results indicate that endothelin-1 may play an important role through which cocaine abstinence affects latent coronary features and therefore potentially warrants further investigations. Furthermore, mediation through noncalcified plaque volumes was non-significant further strengthen our findings that the observed changes in plaque morphology associated with cocaine abstinence are above and beyond the changes that cocaine abstinence causes in plaque volumes.

Structural reorganization of the consensus eigen radiomic feature network

Detailed results are presented in supplemental material. In brief, additional to up or downregulating different elements of the network, interventions or changes in the environment may result in a significant rewiring of the biological network [34]. In abstinent individual we saw that a model considering one changepoint provided the best model fit (figure 5a) as compared to non-abstinent individuals where all statistics supported a model without any changepoints in network structure. Plotting the node positions in latent space, one can appreciate similarities between abstinent and non-abstinent individuals at the first time regime which corresponds to the baseline timepoint (figure 5b and 5g; e.g. brown, royal blue, blue and cyan nodes being clustered together). While latent node positions significantly change in case of abstinent individuals (figure 5c), the relative positions of the eigen radiomic features does not change considerably in non-abstinent participants (figure 5h), only showing a rotation in latent space. Plotting the value of the network generation rule at each timepoint for the corresponding latent dimensions, one can observe a clear divergence in the value of the rule parameter over time in case of abstinent individuals (figure 5d), but not in non-abstinent individuals (figure 5i). Plotting the posterior probability of the given network state being part of the first or second time regime, for abstinent individuals, there is a clear shift in probabilities strengthening the finding of a change in network structure over time in these individuals (figure 5e), but not in non-abstinent participants (figure 5j). These results indicate that cocaine abstinence, not only significant

affects given elements of the latent coronary plaque structure network, but it also results in a significant rewiring of the radiomics network.

DISCUSSION

Advancements in imaging hardware allow visualization of pathologies in-vivo with unprecedented detail. With hard clinical endpoint being scarce due to advancements in medical therapies, surrogate volumetric imaging markers are being used to evaluate the efficacy of therapeutical interventions [5; 6]. However, we do not know whether simple volumetric characteristics are the best surrogates of hard clinical end-points as they hold limited information regarding lesion composition or structure. Radiomics is increasingly being used to quantitatively describe lesion morphology, and has provided insights into pathologies that are not possible using visual assessment of radiological images [10]. Nevertheless, reproducibility issues and redundancy in the parameters hinder the use of individual radiomic features to assess temporal changes in the structure of pathologies [35–37].

In this study we show that using network analysis, we are able to utilize the scale free topology of radiomic feature to provide a flexible framework for the temporal assessment of changes in lesion morphology. Our proposed methodology utilizes the redundancy in the radiomic features to provide highly robust latent descriptors of lesion phenotypes. Our proposed framework is able to analyze cross-sectional and also temporal data, therefore providing a flexible solution for different situations. Furthermore, our implemented methods are inherently able to handle missing data and hierarchical data sources, therefore being ideal for different clinical settings.

In a proof-of-concept implementation, we showed that utilizing the precision phenotyping capabilities of radiomics with the described workflow, we were able to identify latent coronary atherosclerotic morphological features which changed after individuals became abstinent to cocaine use, even after correcting for clinical risk factors and changes in plaque volumes. Using mediation analyses we found that these effects were mediated through serum endothelin-1 levels, which warrants further investigation. Furthermore, using network changepoint analysis, we showed that not only did cocaine abstinence change the values of specific consensus eigen radiomic features, but it also changed the wiring of the radiomic feature network, indicating more substantial effects on lesion morphology.

Our findings have limitations. First, the study is not a randomized clinical trial. Therefore, the observed effects of cocaine abstinence may not be unquestionably attributable to abstinence. Nevertheless, this does not change our findings regarding the robustness of the derived consensus eigen radiomic features, which show that the proposed methodology may be robustly used to describe lesion morphology from medical images. Also, we do not have follow-up data, therefore the clinical relevance of changes in the observed consensus eigen radiomic features and the rewiring of the radiomics network are unknown. Nevertheless, using the proposed framework, researchers may investigate whether the identified imaging markers may be better surrogates of clinical outcomes where follow-up data is available.

In conclusion, our proposed framework provides a flexible methodology to ascertain longitudinal changes in latent imaging morphological features. This allows researchers to evaluate the effect of therapeutical interventions on lesion structure above and beyond volumetric changes. This may help the identification of new surrogate imaging markers that may be better predictors of later clinical outcomes. Furthermore, this methodology opens up new perspectives in connecting in-vivo imaging findings of disease morphology with risk factors, biomarkers or other -omics data sources and therefore may greatly advance our understanding of pathological processes.

Supplementary Material

Refer to Web version on PubMed Central for supplementary material.

ACKNOWLEDGEMENTS

Research reported in this publication was supported by grants from the US National Institute on Drug Abuse, National Institutes of Health (NIH R01DA12777, R01DA15020, R01DA25524, R01DA035632, R21DA048780, and U01DA040325).

ABBREVIATIONS

ACME	average causal mediation effect
ADE	average direct effect
ASCVD	atherosclerosis cardiovascular disease
CAD	coronary artery disease
CTA	computed tomography angiography
HIV	human immunodeficiency virus
HU	Hounsfield unit
IQR	interquartile ranges
TOM	topological overlap matrix
WGCNA	weighted correlation network analysis

REFERENCES

1. Tarkin JM, Dweck MR, Rudd JHF (2019) Imaging as a surrogate marker of drug efficacy in cardiovascular disease. Heart 105:567–578 [PubMed: 30381320]
2. Collaborators GBDCoD (2018) Global, regional, and national age-sex-specific mortality for 282 causes of death in 195 countries and territories, 1980-2017: a systematic analysis for the Global Burden of Disease Study 2017. Lancet 392:1736–1788 [PubMed: 30496103]
3. Roth GA, Johnson C, Abajobir A et al. (2017) Global, Regional, and National Burden of Cardiovascular Diseases for 10 Causes, 1990 to 2015. J Am Coll Cardiol 70:1–25 [PubMed: 28527533]

4. Williams MC, Earls JP, Hecht H (2021) Quantitative assessment of atherosclerotic plaque, recent progress and current limitations. Journal of Cardiovascular Computed Tomography. 10.1016/j.jcct.2021.07.001
5. AstraZeneca, Thrombolysis in Myocardial Infarction Study G (2023) Efficacy and Safety of MEDI6570 in Patients With a History of Myocardial Infarction,
6. MedImmune LLC, Thrombolysis in Myocardial Infarction Study G (2021) A Study to Evaluate the Safety and Efficacy of MEDI6012 in Acute ST Elevation Myocardial Infarction,
7. Williams MC, Kwiecinski J, Doris M et al. (2020) Low-Attenuation Noncalcified Plaque on Coronary Computed Tomography Angiography Predicts Myocardial Infarction: Results From the Multicenter SCOT-HEART Trial (Scottish Computed Tomography of the HEART). Circulation 141:1452–1462 [PubMed: 32174130]
8. Williams MC, Moss AJ, Dweck M et al. (2019) Coronary Artery Plaque Characteristics Associated With Adverse Outcomes in the SCOT-HEART Study. J Am Coll Cardiol 73:291–301 [PubMed: 30678759]
9. Gillies RJ, Kinahan PE, Hricak H (2016) Radiomics: Images Are More than Pictures, They Are Data. Radiology 278:563–577 [PubMed: 26579733]
10. Kolossvary M, Kellermayer M, Merkely B, Maurovich-Horvat P (2018) Cardiac Computed Tomography Radiomics: A Comprehensive Review on Radiomic Techniques. J Thorac Imaging 33:26–34 [PubMed: 28346329]
11. Kolossvary M, Karady J, Szilveszter B et al. (2017) Radiomic Features Are Superior to Conventional Quantitative Computed Tomographic Metrics to Identify Coronary Plaques With Napkin-Ring Sign. Circ Cardiovasc Imaging 10
12. Kolossvary M, Karady J, Kikuchi Y et al. (2019) Radiomics versus Visual and Histogram-based Assessment to Identify Atheromatous Lesions at Coronary CT Angiography: An ex Vivo Study. Radiology 293:89–96 [PubMed: 31385755]
13. Kolossvary M, Fishman EK, Gerstenblith G et al. (2021) Cardiovascular risk factors and illicit drug use may have a more profound effect on coronary atherosclerosis progression in people living with HIV. Eur Radiol 31:2756–2767 [PubMed: 33660033]
14. Kolossvary M, Park J, Bang JI et al. (2019) Identification of invasive and radionuclide imaging markers of coronary plaque vulnerability using radiomic analysis of coronary computed tomography angiography. Eur Heart J Cardiovasc Imaging 20:1250–1258 [PubMed: 30838375]
15. Kolossvary M, Gerstenblith G, Bluemke DA et al. (2021) Contribution of Risk Factors to the Development of Coronary Atherosclerosis as Confirmed via Coronary CT Angiography: A Longitudinal Radiomics-based Study. Radiology 299:97–106 [PubMed: 33591887]
16. Chen DH, Kolossvary M, Chen S, Lai H, Yeh HC, Lai S (2020) Long-term cocaine use is associated with increased coronary plaque burden - a pilot study. Am J Drug Alcohol Abuse 46:805–811 [PubMed: 32990047]
17. Lai H, Moore R, Celentano DD et al. (2016) HIV Infection Itself May Not Be Associated With Subclinical Coronary Artery Disease Among African Americans Without Cardiovascular Symptoms. J Am Heart Assoc 5:e002529 [PubMed: 27013538]
18. Sandfort V, Bluemke DA, Vargas J et al. (2017) Coronary Plaque Progression and Regression in Asymptomatic African American Chronic Cocaine Users With Obstructive Coronary Stenoses: A Preliminary Study. J Addict Med 11:126–137 [PubMed: 28060223]
19. Lai S, Fishman EK, Lai H et al. (2008) Long-term cocaine use and antiretroviral therapy are associated with silent coronary artery disease in African Americans with HIV infection who have no cardiovascular symptoms. Clin Infect Dis 46:600–610 [PubMed: 19641630]
20. Boogers MJ, Broersen A, van Velzen JE et al. (2012) Automated quantification of coronary plaque with computed tomography: comparison with intravascular ultrasound using a dedicated registration algorithm for fusion-based quantification. Eur Heart J 33:1007–1016 [PubMed: 22285583]
21. Inoue K, Motoyama S, Sarai M et al. (2010) Serial coronary CT angiography-verified changes in plaque characteristics as an end point: evaluation of effect of statin intervention. JACC Cardiovasc Imaging 3:691–698 [PubMed: 20633846]
22. Kolossvary M (2021) RIA: Radiomics Image Analysis Toolbox for Grayscale Images,

23. Zhang B, Horvath S (2005) A general framework for weighted gene co-expression network analysis. Stat Appl Genet Mol Biol 4:Article17
24. Langfelder P, Zhang B, Horvath S (2008) Defining clusters from a hierarchical cluster tree: the Dynamic Tree Cut package for R. Bioinformatics 24:719–720 [PubMed: 18024473]
25. Langfelder P, Horvath S (2008) WGCNA: an R package for weighted correlation network analysis. BMC Bioinformatics 9:559 [PubMed: 19114008]
26. Park JH, Sohn Y (2020) Detecting Structural Changes in Longitudinal Network Data. Bayesian Analysis 15:133–157, 125
27. Galili T (2015) dendextend: an R package for visualizing, adjusting and comparing trees of hierarchical clustering. Bioinformatics 31:3718–3720 [PubMed: 26209431]
28. Fleg JL, Morrell CH, Bos AG et al. (2005) Accelerated longitudinal decline of aerobic capacity in healthy older adults. Circulation 112:674–682 [PubMed: 16043637]
29. Verbeke G, Molenberghs G (2001) Linear Mixed Models for Longitudinal Data. Springer New York
30. Bates D, Mächler M, Bolker B, Walker S (2015) Fitting Linear Mixed-Effects Models Usinglme4. Journal of Statistical Software 67:48
31. Kuznetsova A, Brockhoff PB, Christensen RHB (2017) lmerTest Package: Tests in Linear Mixed Effects Models. Journal of Statistical Software 82:26
32. Tingley D, Yamamoto T, Hirose K, Keele L, Imai K (2014) mediation:RPackage for Causal Mediation Analysis. Journal of Statistical Software 59:38
33. R Core Team (2019) R: A language and environment for statistical computing. R Foundation for Statistical Computing, 4.0.0
34. Luscombe NM, Babu MM, Yu H, Snyder M, Teichmann SA, Gerstein M (2004) Genomic analysis of regulatory network dynamics reveals large topological changes. Nature 431:308–312 [PubMed: 15372033]
35. Meyer M, Ronald J, Vernuccio F et al. (2019) Reproducibility of CT Radiomic Features within the Same Patient: Influence of Radiation Dose and CT Reconstruction Settings. Radiology 293:583–591 [PubMed: 31573400]
36. Berenguer R, Pastor-Juan MDR, Canales-Vazquez J et al. (2018) Radiomics of CT Features May Be Nonreproducible and Redundant: Influence of CT Acquisition Parameters. Radiology 288:407–415 [PubMed: 29688159]
37. Kolossvary M, Javorszky N, Karady J et al. (2021) Effect of vessel wall segmentation on volumetric and radiomic parameters of coronary plaques with adverse characteristics. J Cardiovasc Comput Tomogr 15:137–145 [PubMed: 32868246]

Key points:

1. We propose a general methodology to decompose the latent morphology of lesions on radiological images using a radiomics-based systems biology approach.
2. As a proof-of-principle, we show that 1 year cocaine abstinence results in significant changes in specific latent coronary plaque morphologic features and rewiring of the latent morphologic network above and beyond changes in plaque volumes and clinical characteristics.
3. We found Endothelin-1 levels to mediate these structural changes providing potential pathological pathways warranting further investigation.

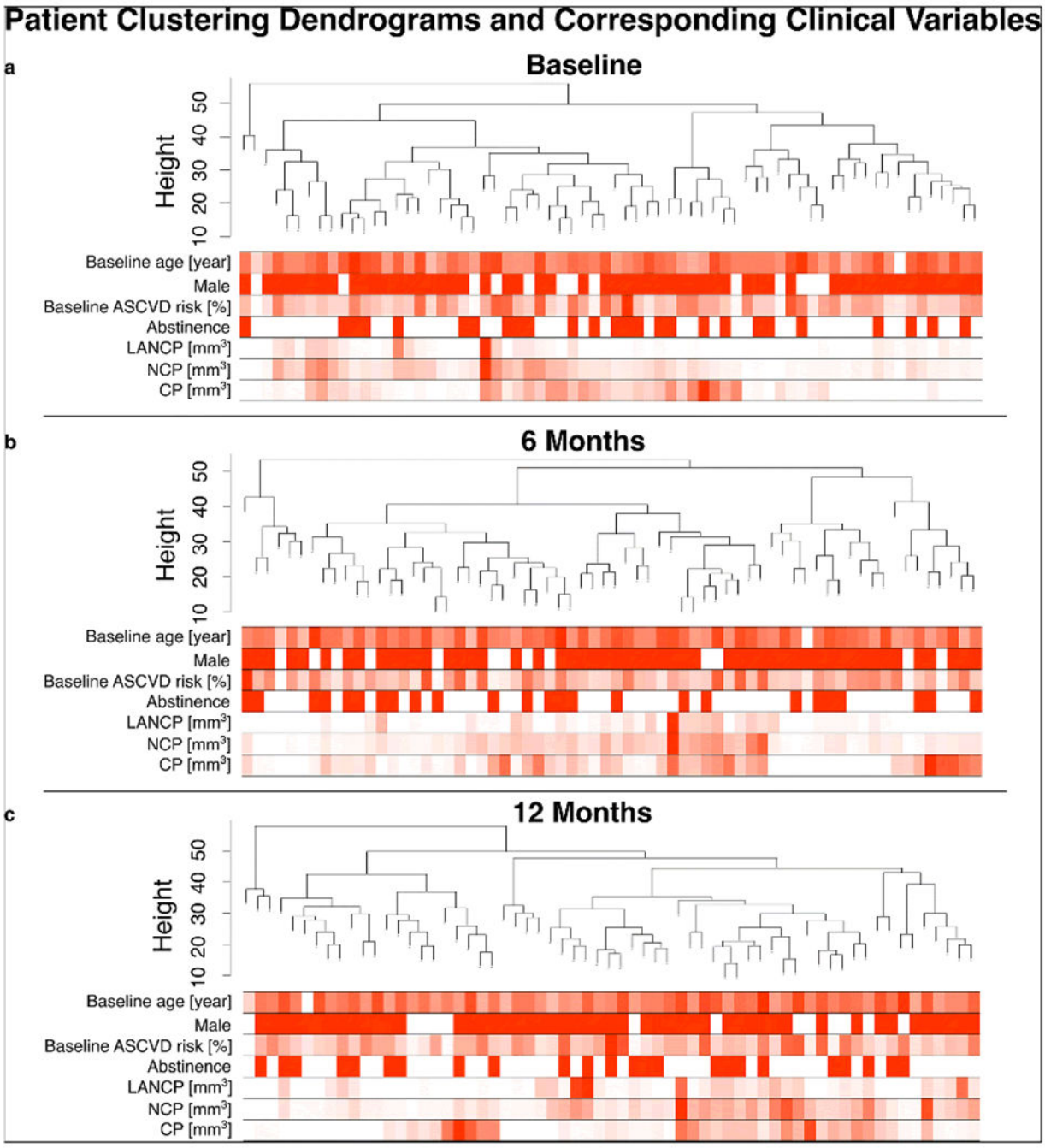

Figure 1.

Hierarchical clustering of patients based on their radiomic profiles and the corresponding clinical values at baseline, 6 months, and 12 months follow-up.

Patient hierarchical clustering dendrograms were created based on the radiomic profiles of the patients at **a)** baseline, **b)** 6 months and **c)** 12 months. Red indicates the value of the given clinical parameter, with red corresponding to the highest value and white corresponding to the lowest value among the individuals. Low cophenetic correlation values between the dendrograms at baseline and 6 months (*cophenetic correlation*=0.42)

and 6 months and 12 months (cophenetic correlation=0.67) indicate substantial changes in radiomic features which result in reorganization of patient similarities.

Abbreviations: ASCVD: atherosclerotic cardiovascular risk, CP: calcified plaque, LANCP: low-attenuation noncalcified plaque, NCP: noncalcified plaque

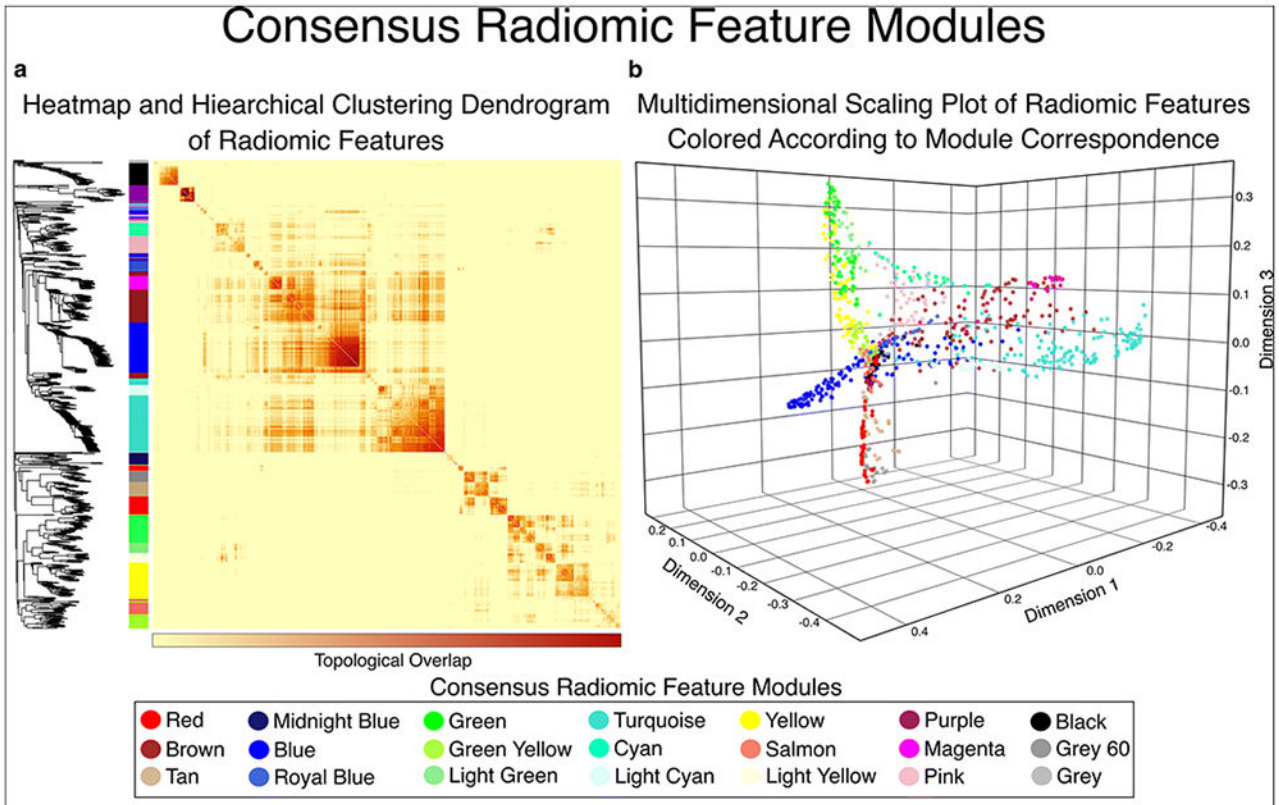

c

Average of Network Quality Characteristics of the Consensus Radiomic Modules

Consensus Radiomic Module	Size	Mean adjacency	log(p)	Mean clustering coefficient	log(p)	Mean correlation	log(p)	Mean maximum adjacency ratio	log(p)	Mean module membership	log(p)	Proportion of variance explained	log(p)
Light Green	24	0.48	-127.14	0.53	-8.42	0.87	-41.61	0.57	-7.48	0.92	-12.70	0.84	-15.24
Yellow	88	0.27	-165.33	0.37	-5.45	0.75	-105.13	0.41	-3.77	0.86	-32.56	0.75	-39.33
Magenta	42	0.39	-173.76	0.63	-30.99	0.74	-44.17	0.62	-18.24	0.86	-15.37	0.77	-20.80
Pink	45	0.27	-68.48	0.37	-2.60	0.76	-47.09	0.40	-1.69	0.85	-14.37	0.74	-16.83
Light Cyan	27	0.37	-73.15	0.47	-5.10	0.81	-39.12	0.50	-4.49	0.89	-13.41	0.80	-15.00
Turquoise	154	0.32	-578.42	0.46	-42.63	0.77	-247.57	0.47	-21.64	0.87	-72.57	0.78	-82.65
Royal Blue	21	0.53	-126.94	0.62	-10.57	0.87	-40.17	0.67	-10.65	0.94	-14.12	0.88	-18.80
Blue	147	0.29	-406.75	0.47	-42.78	0.72	-180.54	0.47	-21.36	0.84	-56.24	0.74	-64.12
Brown	105	0.31	-332.82	0.44	-23.41	0.77	-154.92	0.47	-13.98	0.87	-41.38	0.77	-51.49
Black	51	0.29	-87.20	0.39	-3.54	0.77	-56.76	0.39	-0.88	0.87	-18.81	0.78	-23.27
Green	63	0.38	-240.88	0.46	-12.56	0.82	-100.18	0.53	-14.73	0.90	-30.12	0.82	-36.90
Cyan	30	0.47	-177.26	0.53	-10.48	0.86	-56.02	0.57	-9.86	0.92	-16.39	0.85	-18.56
Light Yellow	22	0.58	-189.90	0.64	-14.29	0.90	-45.20	0.67	-12.55	0.95	-15.28	0.90	-21.16
Red	54	0.33	-160.97	0.47	-12.39	0.76	-65.08	0.54	-12.39	0.87	-21.69	0.77	-26.89
Grey 60	25	0.61	-260.34	0.65	-16.53	0.91	-52.20	0.66	-13.05	0.95	-16.17	0.91	-24.01
Tan	34	0.51	-289.90	0.55	-12.99	0.88	-68.25	0.58	-10.80	0.94	-20.41	0.88	-29.28
Purple	38	0.42	-197.81	0.57	-20.63	0.79	-47.83	0.60	-15.64	0.89	-16.10	0.80	-21.52
Midnight Blue	27	0.16	-11.69	0.37	-1.55	0.62	-15.34	0.48	-3.99	0.79	-7.22	0.63	-6.63
Green Yellow	36	0.24	-34.54	0.36	-0.87	0.73	-39.71	0.42	-1.94	0.86	-14.94	0.74	-15.01
Salmon	32	0.24	-37.12	0.36	-1.39	0.74	-37.21	0.46	-3.82	0.86	-14.50	0.75	-14.05
Grey	16	0.03	0.00	0.32	-0.11	0.19	0.00	0.32	0.00	0.38	0.00	0.25	0.00

Figure 2.

Visual representation of consensus radiomic feature modules.

Using weighted gene co-expression network analysis, we created a consensus topological overlap matrix which provides a representation of the radiomic profile co-expression considering all three timepoints. **a)** shows the topological overlap matrix with the corresponding hierarchical clustering dendrogram on the left. Using the dynamic tree-cut algorithm, we identified 20 consensus radiomic feature modules (grey is used to mark features not allocated to any of the modules). **b)** Plotting the radiomic features in

multidimensional latent space we can appreciate that the features corresponding to the modules are grouped close to each other, while separation between the consensus modules can be observed indicating that the modules represent different latent structural components. **c)** Network quality statistics show that there is high inter-correlation between the elements of each network module. Furthermore, the derived eigen radiomic feature shows high module membership (correlation with the elements of the module) and explains a substantial proportion of the variance of the corresponding features in a given module. These results show that the proposed methodology provides a framework to construct a mathematical representation of the latent structural characteristics of lesions using radiological imaging. Furthermore, this reduces the feature space from 3 timepoints x 1,081 radiomic features to 3 timepoints x 20 consensus eigen radiomic features.

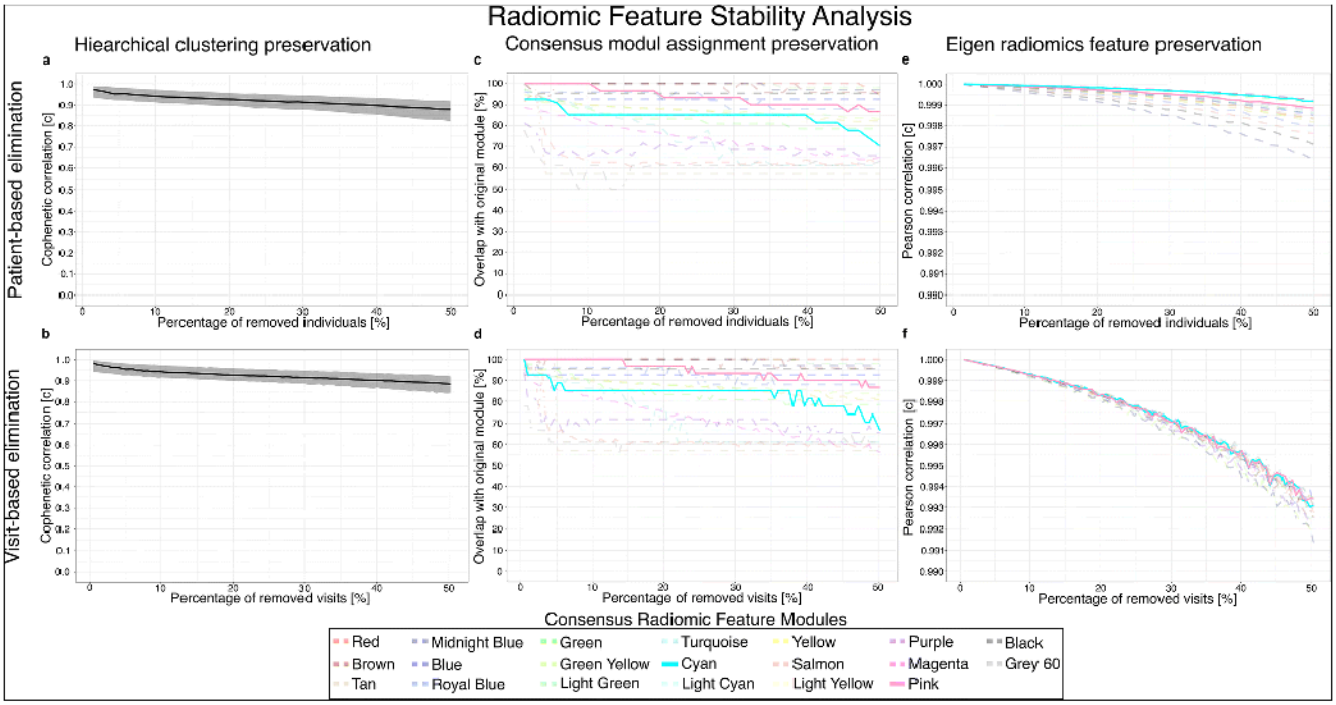

Figure 3.

Stability of radiomic feature modules and consensus eigen radiomic features. Percolation analysis of the radiomic feature network was done by randomly removing data of patients (patient-based elimination) or any of their corresponding visits (visit-based elimination) to analyze the stability of the derived feature modules and consensus eigen features. For each percentage of removed cases, 1,000 random draws were done. The median value of the resulting statistic is presented in the figures. **a, b)** Median and interquartile range of the cophenetic correlation value between the percolated networks and original reference network after excluding patients or visits respectively. **c, d)** Median percentage of overlap in the features assigned to modules derived from the percolated networks and the original 20 feature modules. **e, f)** Median Pearson correlation between the 20 percolated consensus eigen radiomic features and the original consensus eigen radiomic features from the reference network. All preservation statistics highlight the robustness of the derived radiomic feature modules and consensus eigen radiomic features. Values for pink and cyan modules are shown with continuous lines as cocaine abstinence showed a significant association with these two modules.

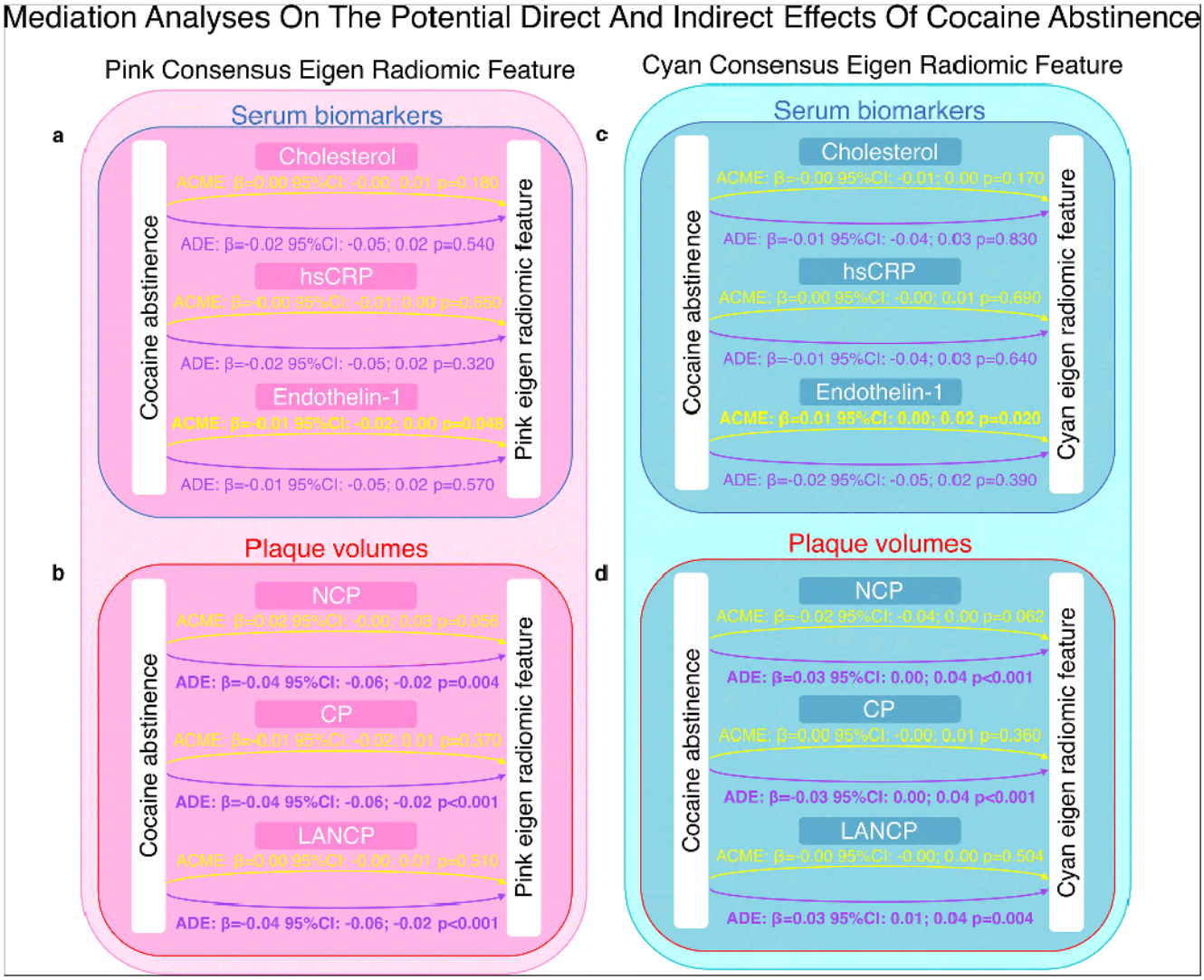

Figure 4.

Mediation analysis on the effects of cocaine abstinence on coronary latent structural features.

Causal mediation analysis was used to estimate the average causal mediation effect (ACME) and the average direct effect (ADE). Even though cocaine abstinence only showed a significant association with endothelin-1 and noncalcified plaque volumes, for completeness the results of all other analyses are presented even though a lack of association with the mediator precludes mediation. **a)** Results for mediation analysis regarding serum biomarkers and the pink consensus eigen radiomic feature. We found a significant ACME for endothelin-1 implying a potential biologically plausible pathway through which cocaine abstinence affects plaque structure. **b)** Results of mediation analysis with regards to plaque volumes. We found no significant ACME for noncalcified plaque volumes further strengthening our findings that cocaine abstinence modifies plaque structure above and beyond its effect on plaque volumes. **c)** Results for mediation analysis with regards to serum biomarkers and the blue consensus eigen radiomic feature. Similar to the pink feature,

endothelin-1 was found to have a significant ACME providing a biological correlate to our findings. **d)** Results for mediation analysis regarding plaque volumes and the blue consensus eigen feature. We found no significant ACME for noncalcified plaque volume showing that the effects of cocaine abstinence on plaque structure are above and beyond the effects on plaque volumes.

Abbreviation: ACME: average causal mediation effect, ADE: average direct effect, CP: calcified plaque volume, hsCRP: high sensitivity C-reactive protein, LANCP: low-attenuation noncalcified plaque, NCP: noncalcified plaque

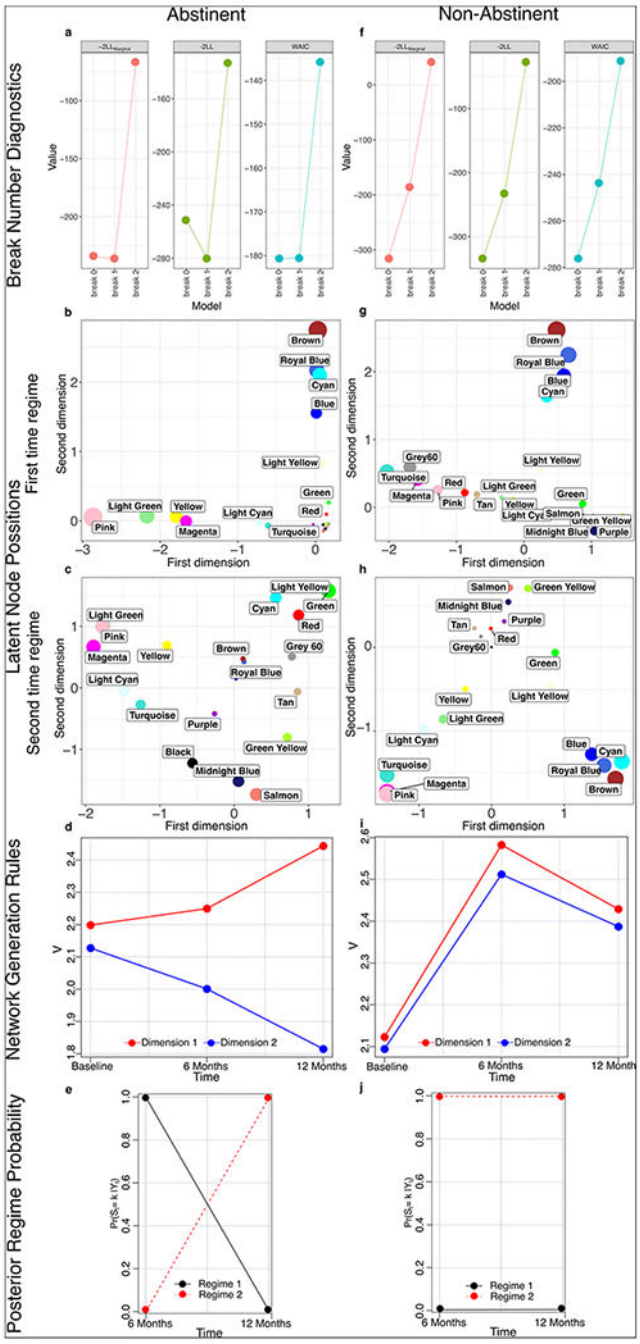

Figure 5.

Network changepoint analysis in abstinent and non-abstinent individuals.

Using Bayesian hidden Markov network changepoint models, we analyzed whether cocaine abstinence resulted in temporal changes in the consensus radiomic feature network topology. **a, f)** Model fit statistics of considering different number of changepoints in the data. In case of abstinent individuals, we found a statistical confirmation of 1 break point, while in non-abstinent individuals, a model without a changepoint had the best fit. **b, g)** Position of consensus radiomic features of abstinent and non-abstinent individuals in the latent

space at the identified first (baseline) time regime. The position of the consensus radiomic features is similar between the two patient groups. **c, h)** Position of consensus radiomic features in latent space in the second time regime (6- and 12-months follow-up). In case of abstinent individuals, significant reorganization of the node positions can be observed, while in non-abstinent participants, the relative node positions are similar to the first time regime, with only a rotation in the latent space. **d, i)** Strength of the network generation rule (V) in each dimension at the different timepoints. A considerable change in the value of V can be observed in abstinent individuals, where the values of V diverge for dimension-1 and -2 following the intervention. However, in case of non-abstinent individuals, V changes synchronously for both dimensions, indicating minimal change in network topology. **e, j)** Posterior probability of being in given regime as a function of time. In case of abstinent individuals there is a clear change in regimes over time, while in case of non-abstinent individual, timepoints correspond to the same regime, indicating there is no changepoint in network topology.

Abbreviation: LL: log-likelihood, $Pr(S_t=k|Y_t)$: posterior probability of given regime state, V: network generation rule, WAIC: Watanabe-Akaike information criterion

Table 1.

Clinical characteristics of cocaine abstinent and non-abstinent at baseline visit.

Characteristic	Abstinent (n = 26)	Non-abstinent (n = 43)	p value
Anthropometrics			
Age [year]	55.0 (53.3, 58.8)	54.0 (51.5, 59.0)	0.33
Male sex [n, %]	20 (76.9%)	36 (83.7%)	0.48
Height [cm]	173 (166, 178)	175 (169, 179)	0.34
Weight [kg]	77.2 (68.4, 94.3)	76.5 (65.7, 93.1)	0.77
BMI [kg/m^2]	27.8 (21.7, 31.4)	24.3 (22.1, 30.7)	0.58
Systolic blood pressure [mmHg]	127.0 (115.5, 139.3)	125.0 (110.0, 139.0)	0.68
Diastolic blood pressure [mmHg]	75.5 (66.0, 83.8)	72.0 (68.0, 81.0)	0.68
African American race [n, %]	24 (92.3%)	40 (93.0%)	0.91
Risk factors			
Hypertension [n, %]	6 (23.1%)	11 (25.6%)	0.82
Diabetes [n, %]	1 (3.8%)	1 (2.3%)	0.72
Cigarette smoking [n, %]	20 (76.9%)	39 (90.7%)	0.12
Alcohol use [n, %]	25 (96.2%)	41 (95.3%)	0.87
Family history of CAD [n, %]	5 (19.2%)	14 (32.6%)	0.23
ASCVD risk [n, %]	10.3 (8.4, 14.4)	10.9 (6.9, 18.6)	0.94
ASCVD risk <7.5% [n, %]	4 (15.4%)	12 (27.9%)	0.23
Statin use [n, %]	6 (23.1%)	9 (20.9%)	0.83
Annual household income< $10,000 [n, %]	15 (57.7%)	24 (55.8%)	0.88
Lab values			
Total cholesterol [mg/dL]	159.0 (142.3, 184.8)	164.0 (145.0, 198.0)	0.63
LDL-C [mg/dL]	81.5 (63.3, 98.0)	81.0 (59.5, 105.5)	0.98
HDL-C [mg/dL]	51.0 (37.8, 65.0)	55.0 (48.0, 71.0)	0.19
Triglycerides [mg/dL]	115.0 (74.0, 222.0)	105.5 (87.3, 143.3)	0.88
Glucose [mg/dL]	88.5 (78.5, 95.0)	83.0 (76.5, 92.0)	0.30
hsCRP [mg/dL]	2.4 (0.7, 5.0)	2.1 (0.6, 6.0)	0.93
hsCRP≥2 mg/mL [n, %]	14 (53.8%)	22 (51.2%)	0.83
Endothelin-1 [pg/mL]	1.5 (1.2, 2.1)	1.6 (1.0, 2.3)	0.34
HIV associated factors			
Years since HIV was diagnosed [year]	20.8 (14.9, 25.3)	18.7 (14.3, 24.1)	0.52
CD4 count at baseline visit [cells/mm^3]	374.5 (172.3, 560.0)	325.0 (148.5, 615.5)	0.76
HIV RNA undetectable at baseline visit [n, %]	9 (34.6%)	19 (44.2%)	0.43
Coronary plaque characteristics			
Total plaque volume [mm^3]	157.8 (101.4, 270.7)	140.7 (60.5, 273.9)	0.83
Noncalcified plaque volume [mm^3]	115.6 (70.9, 186.9)	97.8 (51.3, 219.3)	0.86
Low-attenuation noncalcified plaque volume [mm^3]	2.6 (0.2, 10.1)	2.6 (0.7, 10.1)	0.60

Characteristic	Abstinent (n = 26)	Non-abstinent (n = 43)	p value
Calcified plaque volume [mm^3]	31.2 (5.5, 62.8)	14.1 (0.00, 57.0)	0.43

Data are presented as median and interquartile ranges or frequency and percentage as appropriate. Continuous variables were compared using the Mann-Whitney test, while categorical parameters were compared using the chi-square test.

Abbreviations: ASCVD: atherosclerotic cardiovascular risk, BMI: body mass index, HDL-C, high density lipoprotein cholesterol, HIV: human immunodeficiency virus, hsCRP: high sensitivity C-reactive protein, LDL-C: low density lipoprotein cholesterol, RNA: ribonucleic acid.

Table 2.

Effect of cocaine abstinence on temporal changes in consensus eigen radiomic features.

Consensus Eigen Radiomic Feature	Estimate	95% confidence interval	p value
Light Green	−0.0387	[−0.0685; −0.0089]	0.0117
Yellow	−0.0227	[−0.0536; 0.0081]	0.1500
Magenta	−0.0155	[−0.0419; 0.0109]	0.2521
Pink	**−0.0410**	**[−0.0649; −0.0171]**	**0.0009**
Light Cyan	−0.0193	[−0.0490; 0.0104]	0.2044
Turquoise	−0.0278	[−0.0550; −0.0005]	0.0472
Royal Blue	0.0032	[−0.0277; 0.0342]	0.8373
Blue	−0.0092	[−0.0422; 0.0239]	0.5878
Brown	0.0029	[−0.0219; 0.0278]	0.8170
Black	0.0150	[−0.0201; 0.0501]	0.4035
Green	0.0092	[−0.0151; 0.0334]	0.4613
Cyan	**0.0256**	**[0.0098; 0.0413]**	**0.0017**
Light Yellow	0.0317	[0.0056; 0.0577]	0.0181
Red	0.0036	[−0.0322; 0.0395]	0.8419
Grey 60	−0.0164	[−0.0506; 0.0178]	0.3478
Tan	−0.0061	[−0.0394; 0.0272]	0.7200
Purple	0.0088	[−0.0106; 0.0282]	0.3736
Midnight Blue	−0.0019	[−0.0339; 0.0300]	0.9057
Green Yellow	0.0032	[−0.0205; 0.0270]	0.7911
Salmon	−0.0129	[−0.0440; 0.0182]	0.4163

Multivariate linear mixed models were corrected for baseline age and atherosclerotic cardiovascular disease risk, sex, calcified, noncalcified, and low-attenuation noncalcified plaque volumes at each timepoint. Bold indicates significant associations at a two-sided corrected p threshold of 0.05/20 = 0.0025.